18

Retranslation of Luminescence Excitation during Cascade Transitions in Hybrid Nanostructures Based on INP/INASP/INP NWs and CDSE/ZNS-TOPO QDs

© A.I. Khrebtov[1], A.S. Kulagina[1,¶], N.V. Sibirev[2], A.N. Yablonskiy[3], A.S. Ruban [4], R.R. Reznik[1,2,5,6], G.E. Cirlin[1,2,5,6], V.V. Danilov[4]

[1] Alferov Federal State Budgetary Institution of Higher Education and Science Saint Petersburg National Research Academic University of the Russian Academy of Sciences, St. Petersburg, Russia
[2] St. Petersburg State University, St. Petersburg, Russia
[3] Institute of Physics of Microstructures, Russian Academy of Sciences, Nizhny Novgorod, Russia
[4] Emperor Alexander I St. Petersburg State Transport University, St. Petersburg, Russia
[5] ITMO University, St. Petersburg, Russia
[6] Institute of Analytical Instrument Making, Russian Academy of Sciences, St. Petersburg, Russia

¶e-mail: a.s.panfutova@gmail.com

Received September 04, 2023
Revised October 13, 2023
Accepted October 27, 2023

The features of photoluminescence (PL) of hybrid nanostructures based on InP/InAsP/InP nanowires array with deposited colloidal CdSe/ZnS-trioctylphosphine oxide quantum dots at increasing pump power have been studied. Pumping was carried out by 10 ps laser pulses duration with 1 MHz repetition rate at 532 nm wavelength in the quasi-resonant region of QDs absorption. It has been established, that PL maximum of the nanostructure shifts hypsochromically with increasing of laser power, revealing a gradual dominance of the bands of its components. This PL manifestation is explained by the cascade filling of excited excitonic states, accompanied by the Auger recombination processes and light quenching. The role of free carriers absorption and energy exchange between excitonic states at high pump intensities is noted, as well as a sharp PL duration reduction associated with an increase of stimulated processes in absorption.

Keywords: spectral kinetics, nanowires, colloidal quantum dots, nonradiative energy transfer, cascade filling of states.

DOI: 10.61011/EOS.2023.10.57763.5536-23

Introduction

Hybrid nanocomposites consisting of several semiconductor nanomaterials recently attract more and more interest due to their potential applicability in optical electronics [1,2]. The modern synthesis methods have noticeably broadened a morphological series of such materials. They are often created by being guided with an idea of combining necessary properties therein, which are typical for the components. Such an approach imparts an additional synergetic essence to the composition, i.e. an initiability of a new quality lacking in the initial components.

The photodynamics of relaxation processes in the semiconductor nanocrystals, including the nanocomposites, can be analyzed with an effective qualitative tool, which is photoluminescence (PL) with time resolution. In many cases, the kinetics of luminescence of the semiconductor nanostructures is featured by polyexponential glow decay, which reflects a complex dynamics of the excited state, but it often results in ambiguity of its interpretation due to lack of stable formalism.

Recently, we have demonstrated producibility of nanocomposite structures, which consist of Si (111) substrate-grown InP nanowires (NWs) with an InAsP nanoinsert (NI) and colloidal CdSe/ZnS quantum dots (QDs) covered with trioctylphosphine oxide (TOPO), thereby recording more than triple increase in NI luminescence intensity within the region of $1.3-1.5\,\mu$m [3]. Exemplified by this composition, the papers [4,5] examine a role of model representation in studying the photodynamics of relaxation of the excited excitons and related PL features in the hybrid semiconductor nanostructures. In particular, it shows that the model of contact quenching well describes the PL decay kinetics of the InAsP nanoinsert. It has also confirmed nonradiative energy transfer between the nanostructure components.

Simultaneously, searching ways of controlling the optical and electron properties of the nanostructures has stimulated works for studying the dependence of these properties on the excitation intensity. For example, some works [6–8] have examined the efficiency of colloidal solutions of CdSe/ZnS-TOPO QDs as a medium for optical limitation. However, the increase in the excitation intensity results in significant amplification of processes of nonradiative Auger recombination and in PL quenching. The search of the ways of blocking Auger recombination is exemplified in the

papers [6,9–14]. The present paper examines the features of PL of the InP/InAsP/InP NW + CdSe/ZnS-TOPO QD hybrid nanostructure at high intensities of one picosecond laser excitation within the range of quasi-resonance QD absorption at the room temperature. These studies provide important information not only about the energy migration processes, but about the features of behavior of carriers in the low-dimensional compound structures as well.

Experimental conditions

The nanowires were synthesized on the Si(III) plates using molecular-beam epitaxy on the Compact 21 unit produced by the Riber company. The NW growth technology is described in detail in the paper [15]. The CdSe/ZnS-TOPO QD solution in toluene with the concentration of about 10^{-2} mol/m^3 was applied onto the substrate with QDs (with the surface density of $3 \cdot 10^8$ cm^{-2}). The morphology of the obtained InP/InAsP/InP NW + CdSe/ZnS-TOPO QD hybrid nanostructure was studied using the transmission electron microscopy, its images are given in the paper [3]. Let us list the typical structural components of one NW of an array of such a nanostructure: InAsP nanoinsert (NI) of the length about 45 nm and the diameter about 10 nm, the InAsP radial quantum well (QW), spanning from the NW base to NI, InP NWs (NanoWire, the average height of the InP NW was 4 μm, the base diameter — 100 nm, the apex diameter — 30 nm), covered by the TOPO ligand with quantum dots evenly distributed in 2–3 rows (QDs) with the average diameter about 4.9 nm.

The spectroscopic studies have used a picosecond laser with the pulse duration about 10 ps and the radiation wavelength of 532 nm as the excitation source. The repetition frequency of the laser pulses was 1 MHz (with a pulse thinner). The radiation was focused in a spot of the diameter about 100 μm by means of a converging lens with the focal distance of 30 cm. The Pl signal was collected by means of an achromatic lens Mitutoyo Plan APO NIR 10x. The PL kinetics was measured using a lattice monochromator *Acton 2300i*, a system for detection of single photons based on a superconducting single-photon detector „Skontel“ and a *TimeHarp* 260 system for time-correlated counting of single photons. The time resolution of the PL detection system was ~ 50 ps. All the PL measurements were performed at the room temperature.

Results and discussion

The results of the spectroscopic studies of Fig. 1 show subsequent domination of the PL bands of the InAsP nanoinsert, the InAsP quantum well and the InP NW array with an increasing pumping power. We specifically note a smooth transition from growth to saturation, which usually belongs to the brightest radiation band related to the InAsP nanoinsert.

The studied hybrid nanostructure has the furthest longwave radiation band in the InAsP nanoinsert with the maximum around 1370 nm, while the NQ radiation is exhibited near 1100 nm, so is InP around 900 nm [16]. The QD luminescence around 630 nm is quenched. As shown previously in [3], the QDs of this structure are a donor of nonradiative transfer of energy to the other nanostructure components as per the Förster mechanism. For more detailed analysis of the PL spectrum components, the experimental data are given both in the linear (Fig. 1, *a–e*) and logarithmic coordinates (Fig. 1, *f–j*). It is interesting to note existence of two maxima in InP radiation around 900 nm at high pumping powers (Fig. 1, *h–j*). The time count starts when the PL intensity started to decline in all the spectra. This representation not only makes all the four maxim of radiation visible at the high pumping powers, but makes it possible to evaluate the approximate decay time of each of them along the spectrum scale (by the distance between the power isolines). Specifically, PL decay of NI (at the wavelength of 1370 nm) has a typical time about 3 ns, the wide band of QD (around 1170 nm) has a typical decay time about 1 ns, while the typical times for the maxima from InP were 300 and 100 ps, respectively, at the wavelengths of 960 and 880 nm. The presence of the two PL maxima of InP is related to the presence of the two spaced structures: the very NWs and the two-dimensional layer deposited on the substrate when growing. The difference in the wavelengths can be explained, on the one hand, by quantum-dimensional effects resulting in shift into the blue band. On the other hand, formation of InP NWs in the other crystal phase can result in the shift of the PL band both into the blue and red band. In our case, the further shortwave signal is emitted by the InP layer, so is the further longwave signal by the InP NWs. The InP NWs emit with a larger wavelength, as the valence conduction band of wurtzite InP at InP is higher by 45 meV [17], so the indirect transition is matched with the wavelength about 960 nm.

The kinetics of luminescence decay is often presented as a sum of the components characterizing each emitting state:

$$I_P(\lambda, t) = \sum_i A_{i,P}(\lambda) e^{-\frac{t}{\tau_i}}, \qquad (1)$$

where $I_P(\lambda, t)$ — the PL intensity at ht give pumping power P at the wavelength λ and at the given time — t; $A_{i,P}(\lambda)$ — the amplitudes reflecting a relative portion of the emitting states in the total kinetics of decay. We assume that each emitting state is matched with one time component τ_i, then the index i in our structure will denote the InP-layer (Layer), the InP-NW, the InAsP QW, the InAsP NI. Therefore, the above-said evaluated decay times were refined by the regression analysis: $\tau_{Layer} = 90$ ps, $\tau_{NW} = 330$ ps, $\tau_{QW} = 1.1$ ns, $\tau_{NI} = 3$ ns. Fig. 2 shows the spectrum dynamics of the relative contribution of each state $A_{i,P}(\lambda)$ into the total kinetics of PL decay of the hybrid nanostructure for each excitation mode.

Fig. 2 clearly shows that the shortest component of 90 ps is observed only within the InP band (Fig. 2, *d*), while

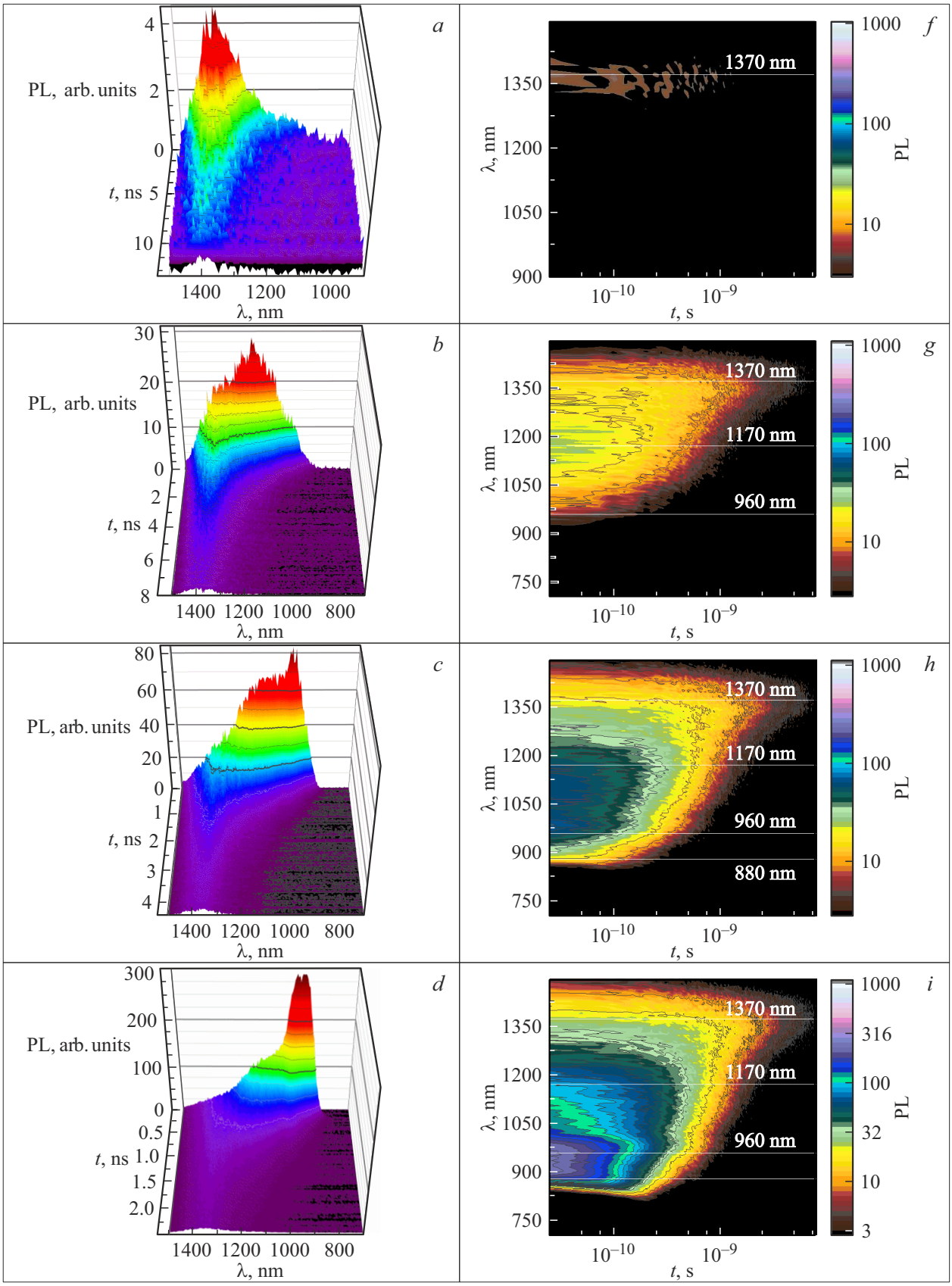

Figure 1. Three-dimension dependencies of the PL intensity of the hybrid InP/InAsP/InP NW,+ CdSe/ZnS-TOPO QD nanostructure on the time and the wavelength, which correspond to the following average pumping powers: (*a*) 0.03 mW; (*b*) 0.3 mW;

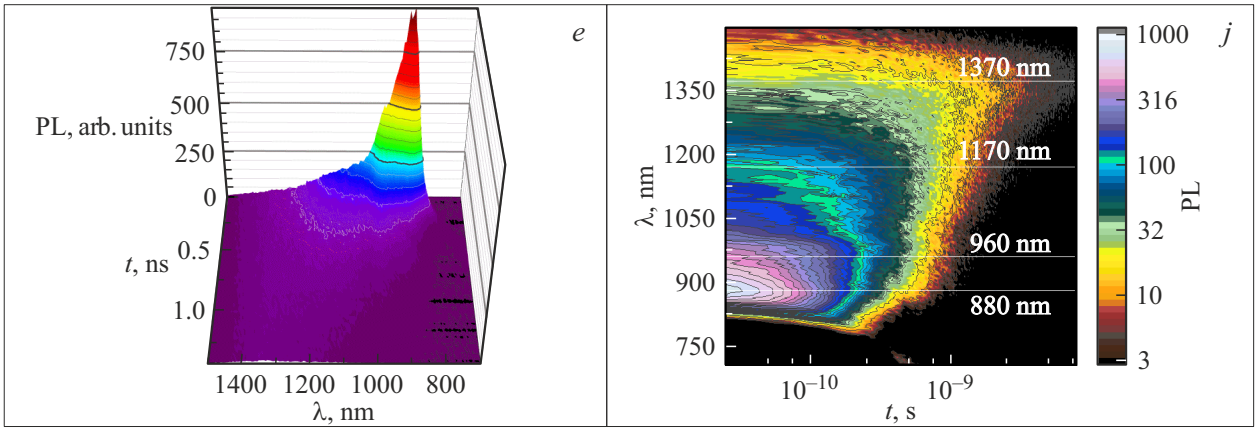

Fig. 1. (*continued*) (*c*) 1 mW; (*d*) 3 mW; (*e*) 8 mW; sweeps of the same spectra in a logarithmic scale in time and the PL intensity are shown under the letters (*f*),(*g*),(*h*),(*i*),(*j*) for each power, respectively.

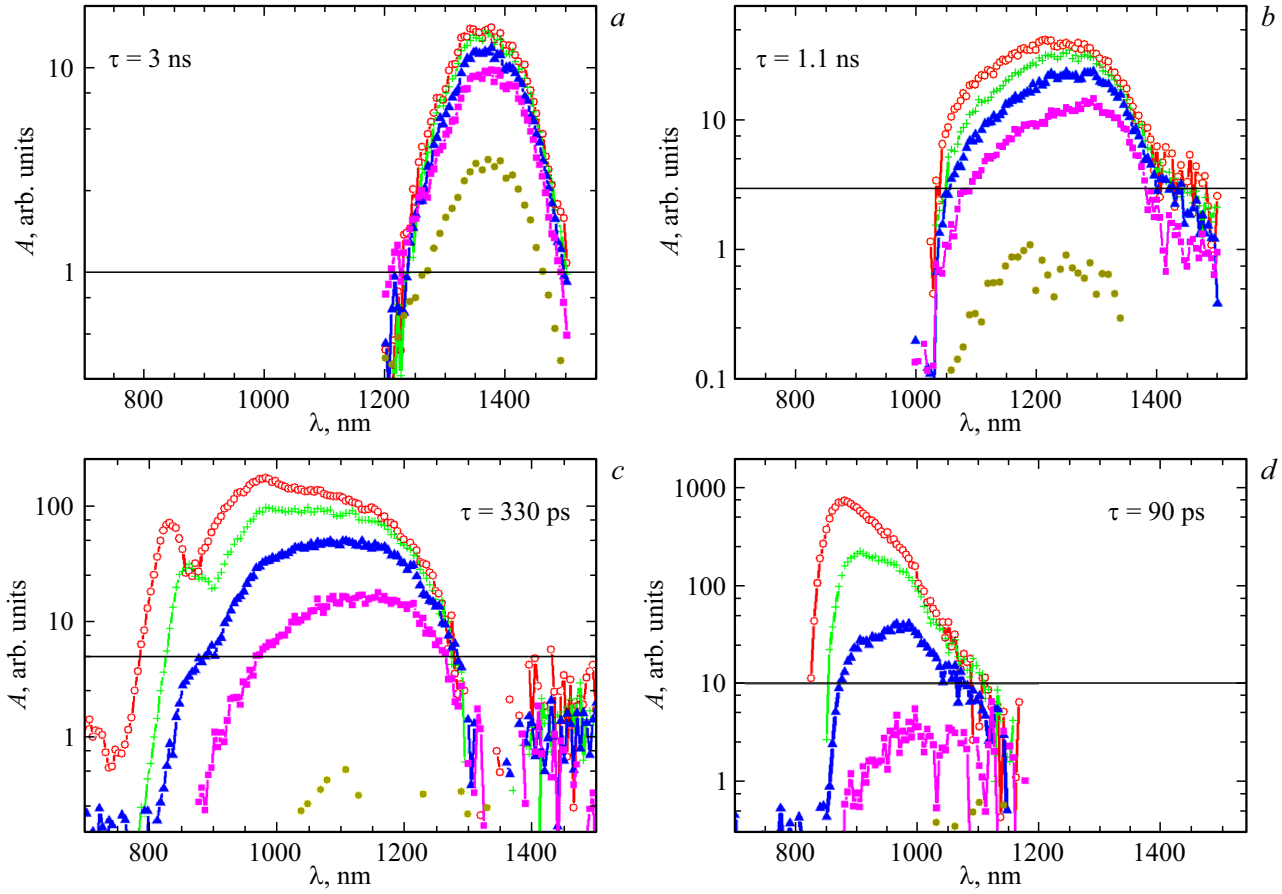

Figure 2. Spectrum dynamics of the PL amplitudes $A_{i,P}(\lambda)$ for each of the four time decay components (*a*) 3 ns; (*b*) 1.1 ns; (*c*) 330 ps; (*d*) 90 ps. The average laser pumping powers are designated in the following order: the filled circles — 0.03 mW; the squares — 0.3 mW; the triangles — 1 mW; the crosses — 3 mW; the empty circles — 8 mW. The horizontal line — the upper evaluation of the error, which is related to an instrument error.

the exponent with decay in 330 ps occurs both in the InP radiation band and the InAsP QD band (Fig. 2, *c*). So, the slowly evanescent exponent is attributed to InP NWs, whereas the quickly evanescent exponent is related to the InP layer deposited on the substrate. The component of the duration of 1.1 ns is typical to a greater extent for QD radiation. The longest component of 3 ns is unambiguously contained in NI radiation only (Fig. 2, *a*). The experiment data enable us to conclude as follows. With the minimum pumping power, it is emitted only by the

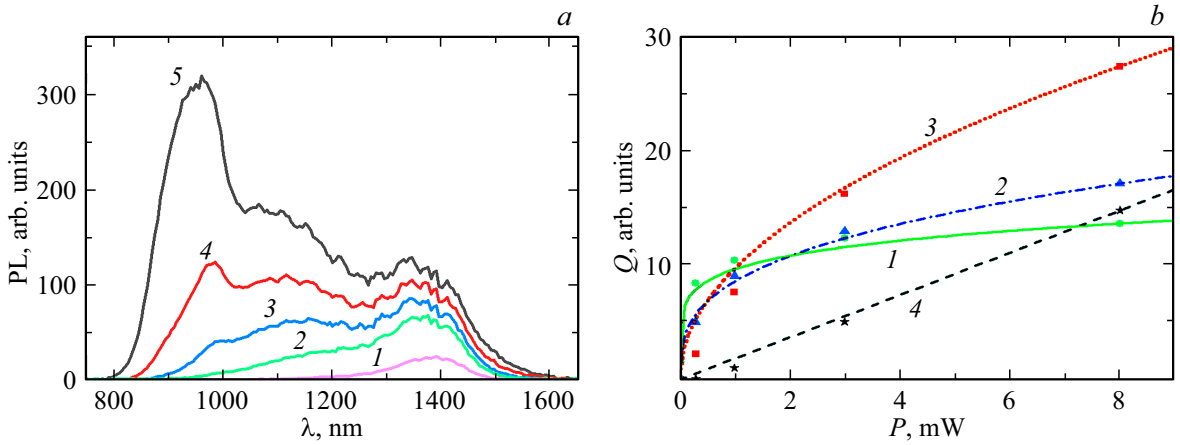

Figure 3. (*a*) Time integral PL spectra of the hybrid nanostructure corresponding to the following pumping intensities (in the pulse): *1* — 0.04 MW/cm^2; *2* — 0.4 MW/cm^2; *3* — 1.3 MW/cm^2; *4* — 3.8 MW/cm^2; *5* — 10.2 MW/cm^2; (*b*) the dependencies of the PL maxima on the laser pumping power for the emitting states: *1* — NI, *2* — QW, *3* — InP NW, *4* — the InP layer and their approximations via the exponential functions: *1* — $Q \sim P^{1/6}$, *2* — $Q \sim P^{1/3}$, *3* — $Q \sim P^{1/2}$, *4* — $Q \sim P$.

InAsP NI at the wavelength about 1370 nm (Fig. 2, *a* and 1, *a*,*f*). Although laser excitation is absorbed by all the components of the hybrid nanostructure, but due to the morphology and the proximity to the resonance band, it is absorbed in the first place by the CdSe/ZnS quantum dots. At the small excitation energies, all the absorbed energy is accumulated at the NW with the least band gap and we observe radiation only from the InAsP NW (Fig. 1, *a*, 1, *f*, 2, *a*). Further, as the laser pump power increases, the excitonic states in the NWs are likely to be completely filled, and the radiative recombination of excitons in the InAsP QW begins to increase (Fig. 2, *b*, *c* and Fig. 1, *g*, *h*). With further increase in the pumping intensity, the similar mechanism is repeated for the emitting states of InP NWs and the InP layer (Fig. 2, *c*, *d*). The InP NW array itself weakly luminesces at the room temperature, but here its radiation becomes prevailing starting from the pumping powers about 3 mW (it corresponds to pulse intensity of 0.4 MW/cm^2). The absence of InP absorption saturation (Figs. 2 and 3) indicates the equality of the absorption cross sections from the ground and first excited states. Let us examine in more detail the processes of filling and relaxation of the interband, exciton and impurity levels in our hybrid nanostructure. At the high intensities of excitation radiation, Auger electrons are actively formed, thereby, inter alia, populating the highest states, the similar mechanism is discussed in the paper [18]. Besides, as noted above, the pumping energy is in a resonance way transferred from the CdSe/ZnS-TOPO QDs to the NI with the least band gap, thereby contributing to its fastest saturation. After that, when increasing intensity of external irradiation, the excess energy received from different channels is redistributed between the higher exciton states, first of the QW, and then of the InP. Suchwise, we suppose occurrence of a cascade „upward" transition contributing to subsequent PL amplification of NI, QD and InP. The cascade nature of the manifestation of luminescence bands of the heterostructure components NI, QW and NW is clearly visible in the time-integrated PL spectra presented in Fig. 3, *a* At the same time, when comparing with Fig. 1, Fig. 3, *a* more clearly exhibits continuing increase in radiation from the InAsP nanoinsert, but, it is obvious that its contribution to the total PL integral becomes less and less. The power-law dependences for the PL maxima, expressed in Q (the emission energy of each state), on the pump power (P) are illustrated in Fig. 3 *b*, corresponding to the four emitting states of the heterostructure; they reveal the saturation nature of each.

A quantitative tool for analyzing relaxation processes, including in semiconductor nanocrystals, is luminescence kinetics. The nature of luminescence decay strongly depends on the pumping intensity and with increase in the latter it quits the monoexponential law. However, even at the low excitation intensities, the studied hybrid InP/InAsP/InP NW,+ CdSe/ZnS-TOPO QD nanostructure is characterized by the polyexponential kinetics of PL decay [5,16]. The paper [16] specifies the following characteristics of the PL kinetics at the low excitation intensities and with all other experiment conditions being equal: at the low temperature of 80 K NI PL decays in a monoexponential way with a rate reciprocal to the constant of 16 ns, the QW PL band has the two components with the durations of 7 and 40 ns, the InP glow declines in less than 2 ns; at the room temperature NI PL has the two time components of 7 and 55 ns, and PLs of QW and InP are quenched. The decay times of the PL signal measured by us in the picosecond excitation at the high pumping powers have turned out to be significantly smaller (Fig. 4), thereby indicating the influence of the light quenching processes. Let us clarify the nature of the PL decay's shortest component of 90 ps. Let the laser radiation be absorbed mainly by CdSe/ZnS-TOPO QDs in all the

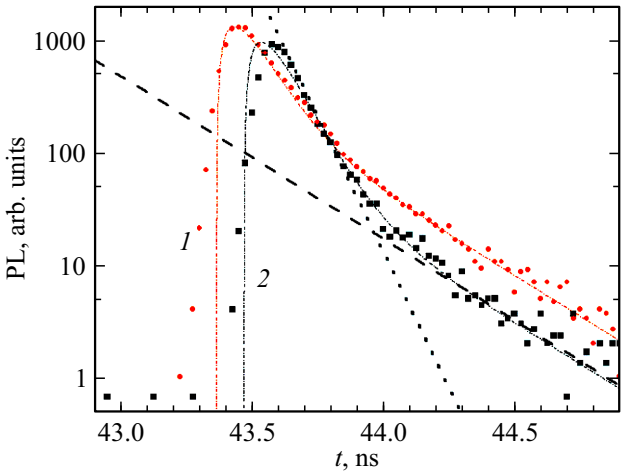

Figure 4. FL kinetics of the hybrid InP/InAsP/InP NW,+ CdSe/ZnS-TOPO QD nanostructure at the pumping power of 8 mW for the two lines of InP radiation: (*1*) the circles — 960 nm, (*2*) the squares — 880 nm. For clarity, the dotted line marks the fast declining exponent with $\tau_{Layer} = 90$ ps, so does the dashed line — the slowly decreasing exponent with $\tau_{NW} = 330$ ps, so does the fine dash-dotted line — approximation in the form of the sum of the four exponents.

cases. It is probable that the energy is transferred from QDs to InP NWs faster than the instrument's time resolution. The process of signal transfer from QDs to the InP layer on the substrate is slower. In this case the kinetics of the signal from the InP layer is described by the equation (2):

$$\frac{dn_{Layer}}{dt} = -\frac{n_{Layer}}{\tau'_{Layer}} + \frac{q_{Layer}}{t_{Layer}}\left(1 - \frac{n_{Layer}}{n_{Layer,max}}\right), \qquad (2)$$

where $q_{Layer} = q_L \exp\left(-\frac{t}{t'_{Layer}}\right)$, n_{Layer} — the population of the InP layer, τ'_{Layer} — the relaxation time of the exciton levels of the InP layer (radiative and nonradiative), q_{Layer} — the population of the CdSe/ZnS-TOPO QDs on the substrate, t_{Layer} — the time of nonradiative transfer of energy from QDs to the substrate, t'_{Layer} — the time of the relaxation processes in the CdSe/ZnS-TOPO QDs on the substrate, $n_{Layer,max}$ — the limit population of the InP layer.

Even in the approximation of the small population $\frac{n_{Layer}}{n_{Layer,max}} \ll 1$ the solution of the equation (2) contains two exponents with the typical times of τ'_{Layer} and t'_{Layer}. In order to evaluate these times, we will evaluate the time to the maximum of the signal after the pumping pulse passed: $t_{max} = \tau'_{Layer} t'_{Layer} \frac{1}{(t'_{Layer} - \tau'_{Layer})} \ln\left(\frac{t'_{Layer}}{\tau'_{Layer}}\right)$. From the properties of this equation it is easy to see that if two characteristic times are very different, then the dependence on the fast component is linear, and on the slow component it is logarithmic. Time t'_{Layer} is not determined directly. However, it can be said for sure that the relaxation time of the exciton levels of the InP layer exceeds 90 ps and concluded that the radiation spectrum of the InP layer is heterogeneously broadened. We attribute the constant itself with a duration of 90 ps to the time of relaxation processes in the CdSe/ZnS-TOPO QD on the substrate. This agrees well with the data of the paper [18].

Due to the quantitative ratio in the studied hybrid nanostructure, the main absorbers of excitation energy include the CdSe/ZnS-TOPO QDs and the InP array. Since at the high pumping intensities the absorption is implemented through the highest excitonic states or the free carriers, then the lower radiative state of InAsP is populated via several channels. The features of the cascade transitions and the role of the processes of energy transfer therein has been noted by many authors. Specifically, the authors of [19] have implemented a heterogeneous structure with a funnel-like change of the band gap width. In this case PL of the highly-lying excitonic states was fully quenched and the red luminescence was abruptly amplified. The studies of the colloidal structures based on the CdTe/CdSe tetrapods [20] by pulse nanosecond excitation have shown bleaching of the exciton absorption band $1Se-1Sh_{3/2}$ stabilization of the intensity of recombination luminescence with increase in the intensity, starting from the level of 2 MW/cm^2 for the CdSe domain and of 5 MW/cm^2 for the entire structure of the tetrapod. Such a process shall result in similar stabilization of the energy flow from the CdSe/ZnS QDs to InAsP NIs in our case, too. The other potential channels for population of the radiative level of NI include relaxation with involvement of defects and energy exchange between the heavy and light holes. The local phonon modes of the traps amplify the hole-phonon bond. The heterogeneity of the nanostructure causes traps at the interfaces, which are also involved in the processes of capture and energy exchange. In turn, the main channel of nonradiative deactivation of the lower radiative state in nanostructures is considered to be the enhancement of Auger recombination. In our case, the Auger exchange is accompanied by light quenching and absorption by the free carriers during intra-band exciton excitation (thereby enabling the use of the Drude model for calculation of the corresponding sections of extinction). All these processes are directed oppositely to the longitudinal relaxation, which shall result in dynamic equilibrium and, as a result, bleaching of the exciton transitions 1Se, $1Sh_{3/2}$ and PL saturation. As specified in [21], at the high pumping intensities, due to Auger heating [22], the unoccupied high-energy excitonic states exhibit an effect of cascade filling of the phase space of the excitons. It is obvious that for various luminescent components of the nanostructure it will be filled at various excitation intensities, which is indicated by individual exciton glow bands of NIs, QDs and InP observed in the PL spectra. Fig. 5 shows a diagram of the energy levels of our hybrid nanostructure, which illustrates the idea of cascade filling of the excitonic states. Initially, according to Kasha's rule, emission occurs from the lower excited level, which in the case of the InP/InAsP/InP NWs+CdSe/ZnS-TOPO QDs composition is the exciton state corresponding to the transitions $1Se-1Sh_{3/2}$ of the InAsP nanoinsert (on Fig. 5 stage *A*). The increase in the level of optical excitation results in bleaching of the exciton

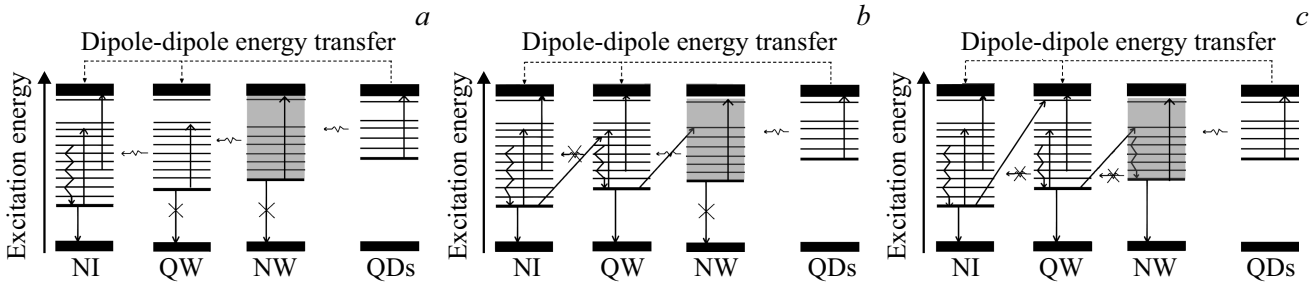

Figure 5. Energy diagram of the photodynamics of excitation and relaxation of the excitons in the hybrid InP/InAsP/InP + CdSe/ZnS-TOPO QD nanostructure. *a*) Processes at unsaturated the lower excitonic state of NI; *b*) Processes during saturation of the lower excitonic state of NI. *c*) Processes during saturation of the NI and QW states. Upward straight arrows — absorption from the excited states (light quenching and absorption by the free carriers). Downward straight arrows — PL, crossed arrows — irrelevant processes. Downward wavy arrows — relaxation processes. Inclined arrows — Auger processes. Dotted arrows — resonance energy transfer. Horizontal wavy arrows — contact energy transfer.

absorption band $1Se-1Sh_{3/2}$ InAsP NI and its PL saturation. Various nonlinear processes compete simultaneously in the heterostructure: light quenching, Auger processes, Drude transitions, etc. (see. Fig. 5). PL from the QW radiative level (the stage *B*) becomes dominant at the excitation intensities which exceed the absorption saturation intensity of the NI InAsP transition. These are the same excitonic states $1Se-1Sh_{3/2}$, but they belong to the more highly-energetic components of the heterostructure. Thus, with increase in the intensity, the bleaching process is repeated for the excitonic states $1Se-1Sh_{3/2}$ of the heterostructure QW. For the stage *C*, the process of absorption saturation is not achieved in the conditions of our experiment.

Taking into account several assumptions, the relaxation model of Fig. 5 can be written as the following system of equations (3):

$$q_{NW} = q_0 \exp\Big(-t\Big[\frac{1}{t_{NW}} + \frac{1}{t_{QW}} + \frac{1}{t_{NW'}}\Big]\Big),$$

$$\frac{dn_{NW}}{dt} = -\frac{n_{NW}}{\tau'_{NW}} + \frac{q_{NW}}{t_{NW}}\Big(1 - \frac{n_{NW}}{n_{NW,max}}\Big) - \\ -\frac{n_{NW}}{\tau_{QW,NW}}\Big(1 - \frac{n_{QW}}{n_{QW,max}}\Big) - \frac{n_{NW}}{\tau_{NW,NI}}\Big(1 - \frac{n_{NI}}{n_{NI,max}}\Big),$$

$$\frac{dn_{QW}}{dt} = -\frac{n_{QW}}{\tau'_{QW}} + \frac{q_{NW}}{t_{QW}}\Big(1 - \frac{n_{QW}}{n_{QW,max}}\Big) + \\ +\frac{n_{NW}}{\tau_{QW,NW}}\Big(1 - \frac{n_{QW}}{n_{QW,max}}\Big) - \frac{n_{QW}}{\tau_{NI,QW}}\Big(1 - \frac{n_{NI}}{n_{NI,max}}\Big),$$

$$\frac{dn_{NI}}{dt} = -\frac{n_{NI}}{\tau'_{NI}} + \frac{n_Q W}{\tau_{NI,QW}}\Big(1 - \frac{n_{NI}}{n_{NI,max}}\Big) + \frac{n_{NW}}{\tau_{NW,NI}} \times \\ \times\Big(1 - \frac{n_{NI}}{n_{NI,max}}\Big). \qquad (3)$$

Since the PL spectrum longer than 1300 nm does not contain fast exponents 90 ps and 330 ps (Fig. 2, *c*, *d*), we neglected the terms associated with energy transfer from QD CdSe/ZnS-TOPO to NV. The first equation of the system (3) describes the population of the levels in the quantum dots deposited on the NWs after radiation absorption. Here t_{NW}, t_{QW} — the times of transfer of energy from QDs to InP NWs and InAsP QWs, respectively, $t_{NW'}$ — the times of the other processes of excitation relaxation in QDs. The equations (2–4) of the system (3) describe the population of the level in InP NW, InAsP QW and InAsP NI, respectively. Here n_{NW}, n_{QW}, n_{NI} — the populations of the levels in InP NW, InAsP QW and InAsP NI, $n_{NW,max}$, $n_{QW,max}$, $n_{NI,max}$ — the limit populations of the respective levels. $\tau_{i,j}$ — the time of nonradiative transfer of energy from one object j to another $i(i, j : NW, QW, NI)$. τ'_{NW}, $\tau_{QW'}$, τ'_{NI} — the relaxation times of the exciton levels of InP NW, InAsP QW and InAsP NI, the radiative one and the nonradiative one, without taking into account the transitions.

The measured decay times of the heterostructure components $\tau_{NW} = 330$ ps, $\tau_{QW} = 1.1$ ns, $\tau_{NI} = 3$ ns are related to the parameters in the equations of the system (3) as follows:

$$\frac{1}{\tau_{NW}} = \frac{1}{\tau'_{NW}} + \frac{1}{\tau_{QW,NW}} + \frac{1}{\tau_{NI,NW}},$$
$$\frac{1}{\tau_{QW}} = \frac{1}{\tau'_{QW}} + \frac{1}{\tau'_{NI,QW}},$$
$$\frac{1}{\tau_{NI}} = \frac{1}{\tau'_{NI}}. \qquad (4)$$

Only the relaxation time of the states in NI $\tau'_{NI} = 3$ ns can be determined directly from the system of equations (4). Nevertheless, taking into account the decay constants of all the states of the hybrid nanostructure at the low pumping densities [16] makes it possible to perform the following evaluations: $\tau_{NI,QW} = 1.2$ ns, $\tau'_{QW} > 10$ ns, $\tau'_{NW} \approx 1$ ns, $\tau_{QW,NW} \approx 650$ ps, $\tau_{NI,NW} \approx 2$ ns.

This structure may be interesting when creating a tunable source of radiation in the visible and near IR ranges.

Conclusion

The study has detected a hypsochromic shift of the PL maximum during increase in the laser pumping power,

which illustrates subsequent domination of the radiation bands of the heterostructure components at the room temperature. This shift is caused by bleaching of its ground states during intra-band exciton excitation. The photoluminescence saturation for NI and QW is related by us to the effect of filling of the excitonic states, including by Auger recombination at the high pumping intensities. Performed analysis showed the significant reduction in the PL decay times of each emitting state of the hybrid nanostructure compared to the linear excitation mode, and also revealed the contribution and features of the PL kinetics of the InP layer on the substrate. The times of nonradiative transfer of energy from NW to QW, from NW to NI and from QW to NI have been evaluated. The proper relaxation times of the excitonic levels of InAsP QW and InAsP NI have been evaluated for the formed hybrid structure. The exciton-exciton interaction and the phonon-caused cascade relaxation of the free electrons and holes have defined the dynamics of resonance-excited excitons.

Acknowledgments

The authors would like to express their gratitude to E.N. Bodunov for his interest and attention to the study.

Funding

The semiconductor nanowires were synthesized with the financial support of the Ministry of Science and Higher Education in the part of the State Assignment № 0791-2023-0004. The deposition of quantum dots onto the surface of nanowires was carried out with the financial support of the Ministry of Science and Higher Education of the Russian Federation, the research project №2019-1442 (the research topic code FSER-2020-0013). The optical properties of the hybrid nanostructures were studied under the State Assignment №0030-2021-0019 using the equipment belonging to CUC „Physics an technology of micro- and nanostructures“ of the IFM RAS. The optical properties of the hybrid nanostructures were simulated with the financial support of St. Petersburg State University within the research grant №94033852.

Conflict of interest

The authors declare that they have no conflict of interest.

References

[1] K. Rajeshwar, N.R. Tacconi, C.R. Chenthamarakshan. Chem. Mater., **13** (9), 2765 (2001). DOI: 10.1021/cm010254z
[2] J. Li, J.Z. Zhang. Coord. Chem. Rev., **253** (23–24), 3015 (2009). DOI: 10.1016/j.ccr.2009.07.017
[3] A.I. Khrebtov, R.R. Reznik, E.V. Ubyivovk, A.P. Litvin, I.D. Skurlov, P.S. Parfenov, A.S. Kulagina, V.V. Danilov, G.E. Cirlin. Semicond., **53** (9), 1258 (2019). DOI: 10.1134/S1063782619090082.
[4] A.S. Kulagina, A.I. Khrebtov, R.R. Reznik, E.V. Ubyivovk, A.P. Litvin, I.D. Skurlov, G.E. Cirlin, E.N. Bodunov, V.V. Danilov. Opt. Spectr. **128** (1), 119 (2020). DOI: 10.1134/S0030400X20010129.
[5] A.I. Khrebtov, A.S. Kulagina, V.V. Danilov, E.S. Gromova, I.D. Skurlov, A.P. Litvin, R.R. Reznik, I.V. Shtrom, G.E. Tsyrlin. FTP, **54** (9), 952 (2020) (in Russian). DOI: 10.21883/FTP.2020.09.49838.32 [A.I. Khrebtov, A.S. Kulagina, V.V. Danilov, E.S. Gromova, A.P. Litvin, I.D. Skurlov, R.R. Reznik, I.V. Shtrom, G.E. Cirlin. Semicond., **54** (9), 1141 (2020). DOI: 10.1134/S1063782620090158].
[6] V.V. Danilov, A.S. Panfutova, A.I. Khrebtov, S. Ambrosini, D.A. Videnichev. Opt. Lett., **37** (19), 3948 (2012). DOI: 10.1364/OL.37.003948
[7] S. Valligatla, K.K. Haldar, A. Patra, N.R. Desai. Opt. Laser Technol., **84**, 87 (2016). DOI: 10.1016/j.optlastec.2016.05.009
[8] V.V. Danilov, A.I. Khrebtov, A.S. Panfutova, G.E. Cirlin, A.D. Bouravleuv, V. Dhaka, H. Lipsanen. Tech. Phys. Lett., **41** (2), 120 (2015). DOI: 10.1134/S1063785015020066
[9] V.I. Klimov. J. Phys. Chem. B, **104**, 6112 (2000). DOI: 10.1021/jp9944132
[10] V.V. Vistovskyy, A.V. Zhyshkovych, O.O. Halyatkin, N.E. Mitina, A.S. Zaichenko, P.A. Rodnyi, A.S. Voloshinovskii. J. Appl. Phys., **116** (5), 054308 (2014). DOI: 10.1063/1.4892112
[11] V.I. Klimov. Annu. Rev. Condens. Matter Phys., **5**, 285 (2014). DOI: 10.1146/annurev-conmatphys-031113-133900
[12] K. Kyhm, J.H. Kim, S.M. Kim, H.S. Yang. Opt. Mater., **30** (1), 158 (2006). DOI: 10.1016/j.optmat.2006.11.036
[13] L.A. Padilha, J.T. Stewart, R.L. Sandberg, W.K. Bae, W.K. Koh, J.M. Pietryga, V.I. Klimov. Nano Lett., **13** (3), 1092 (2013). DOI: 10.1021/nl304426y
[14] A.I. Khrebtov, A.S. Kulagina, V.V. Danilov, A.S. Dragunova, K.P. Kotlyar, R.R. Reznik, G.E. Cirlin. J. Opt. Tech., **89** (5), 298 (2022). DOI: 10.1364/JOT.89.000298
[15] R.R. Reznik, G.E. Cirlin, I.V. Shtrom, A.I. Khrebtov, I.P. Soshnikov, N.V. Kryzhanovskaya, E.I. Moiseev, A.E. Zhukov. Tech. Phys. Lett., **44** (3), 112 (2018). DOI: 10.1134/S1063785018020116
[16] A.I. Khrebtov, V.V. Danilov, A.S. Kulagina, R.R. Reznik, A.P. Litvin, I.D. Skurlov, F.M. Safin, V.O. Gridchin, D.S. Shevchuk, S.V. Shmakov. Nanomat., **11** (3), 640 (2021). DOI: 10.3390/nano11030640
[17] K. Ikejiri, Yu. Kitauchi, K. Tomioka, J. Motohisa, T. Fukui. Nano Lett., **11**, 4314 (2011). DOI: 10.1021/nl202365q
[18] V.V. Danilov, A.S. Kulagina, N.V. Sibirev. Appl. Opt., **57** (28), 8166 (2018). DOI: 10.1364/AO.57.008166
[19] L. Franz, T. Klar, T.A. Schietinger, S. Rogach, J. Feldmann. Nano Letters., **4** (9), 1599 (2004). DOI: 10.1021/nl049322h
[20] A.D. Golinskaya, A.M. Smirnov, M.V. Kozlova, E.V. Zharkova, R.B. Vasiliev, V.N. Mantsevich, V.S. Dneprovskii. Results Phys., **27**, 104488 (2021). DOI: 10.1016/j.rinp.2021.104488
[21] A.M. Smirnov, A.D. Golinskaya, B.M. Saidzhonov, V.N. Mantsevich, V.S. Dneprovskii, R.B. Vasiliev. J. Lumin., **229**, 11768245 (2021). DOI: 10.1016/j.jlumin.2020.117682
[22] D.J. Trivedi, L. Wang, O.V. Prezhdo. Nano Lett., **15** (3), 2086 (2015). DOI: 10.1021/nl504982k

Translated by M.Shevelev